Self-consistent analysis of single-particle excitations in a spin-density-wave antiferromagnet

J. Altmann, W. Brenig, Arno P. Kampf, E. Müller-Hartmann

Angaben zur Veröffentlichung / Publication details:

Altmann, J., W. Brenig, Arno P. Kampf, and E. Müller-Hartmann. 1995. "Self-consistent analysis of single-particle excitations in a spin-density-wave antiferromagnet." *Physical Review B* 52 (10): 7395–7401. https://doi.org/10.1103/physrevb.52.7395.

Self-consistent analysis of single-particle excitations in a spin-density-wave antiferromagnet

J. Altmann, W. Brenig, A.P. Kampf, and E. Müller-Hartmann
Institut für Theoretische Physik, Universität zu Köln, Zülpicher Strasse 77, D-50937 Köln, Germany
(Received 14 March 1995)

We present the results of a self-consistent weak-coupling calculation for the renormalized single-particle properties in an itinerant antiferromagnet. Multiple spin-wave excitations accompany the carrier motion and lead to incoherent contributions to the electronic spectrum. We evaluate the quasiparticle spectral weight and energy dispersion. In agreement with strong-coupling theories we find the minimum of the dispersion of the quasihole energy to have momentum $(\pm\pi/2, \pm\pi/2)$ and the dispersion to be flat around the corners of the Brillouin zone. Very good agreement is achieved with available exact diagonalization data.

I. INTRODUCTION

In recent years the study of hole motion in an antiferromagnetically (AF) correlated environment has been the focus of theoretical work on weakly doped high-temperature superconductors.[1] The AF insulating parent compounds have been described in terms of the spin-$\frac{1}{2}$ Heisenberg model on a square lattice or the spin-density-wave (SDW) state of the Hubbard model at half-filling. In the itinerant SDW state the electronic hopping motion is accompanied by the emission and absorption of collective spin-wave excitations strongly renormalizing the single-particle spectrum. Similar pictures have been developed and are assumed to be relevant for the Hubbard model or the t-J model when doped slightly away from half-filling where finite-range AF spin correlations still persist.

Complementary to numerical simulations self-consistent diagrammatic schemes have been used, especially for the t-J model,[2–4] to calculate the renormalization of single-particle properties due to coupling of the charge carriers to spin fluctuations. In particular, the spin-fluctuation dressing leads to low-frequency contributions to the optical conductivity[5] and may be the origin of the midinfrared band observed in the optical spectra of $La_{2-x}Sr_xCuO_4$.[6]

In this paper we report the results of a self-consistent weak-coupling evaluation of the electronic spectrum based on the SDW state of the half-filled Hubbard model on a square lattice.

We calculate the single-particle self-energy taking into account multiple exchange of transverse-spin excitations. In solving the self-energy equations we go beyond previous analyses which either use a one-loop approximation for the self-energy[7–9] or solve the self-energy equations in the strong-coupling limit.[10]

Our results show a considerable shift of spectral weight from the quasihole peak to the incoherent part of the spectrum. This effect is strongest in the center of the Brillouin zone. The bandwidth and the single-particle excitation gap are found to be strongly renormalized. In correspondence with results for the t-J model,[4,11] the minimum of the quasihole energy is located at the momenta $(\pm\frac{\pi}{2}, \pm\frac{\pi}{2})$ with a very flat dispersion around the corners of the magnetic Brillouin zone (MBZ). The density of states displays two separate contributions of distinct origin: the valence and conduction band of the propagating quasiparticles and for intermediate-coupling strength additional spectral intensity on the energy scale of the Hubbard interaction U.

The paper is organized as follows: In Sec. II we recollect the basic steps of the SDW formalism for the Hubbard model and calculate the transverse-spin susceptibility in the random-phase approximation (RPA). In Sec. III we derive the self-energy equations for a single hole in the SDW state. We discuss the results of their numerical solution in Sec. IV.

II. SDW FORMALISM AND SPIN-WAVE EXCITATIONS

We start from the standard one-band Hubbard model[12] on a square lattice

$$H = \sum_{\mathbf{k},\sigma} \epsilon_{\mathbf{k}} c^{\dagger}_{\mathbf{k}\sigma} c_{\mathbf{k}\sigma} + \frac{U}{N} \sum_{\mathbf{k},\mathbf{l},\mathbf{q}} c^{\dagger}_{\mathbf{k}\uparrow} c^{\dagger}_{\mathbf{q}-\mathbf{k}\downarrow} c_{\mathbf{q}-\mathbf{l}\downarrow} c_{\mathbf{l}\uparrow}. \quad (1)$$

Here $c^{(\dagger)}_{\mathbf{k}\sigma}$ destroy (create) fermions of momentum $\mathbf{k}$ and spin σ. N is the number of sites and U denotes the on-site Hubbard repulsion. The bare tight-binding dispersion $\epsilon_{\mathbf{k}}$ is given by $\epsilon_{\mathbf{k}} = -2t(\cos k_x + \cos k_y)$ where t is the hopping integral and the lattice constant is set to unity. At half-filling the nesting property $-\epsilon_{\mathbf{k}} = \epsilon_{\mathbf{k}+\mathbf{Q}}$ of the tight-binding dispersion leads to an instability of the noninteracting Fermi sea and favors the formation of a commensurate SDW state with a modulation wave vector $\mathbf{Q} = (\pi, \pi)$. On the mean-field level this is described by a Hartree-Fock (HF) factorization of (1) (Ref. 13)

$$H_{\mathrm{MF}} = \sum_{\mathbf{k},\sigma} \epsilon_{\mathbf{k}} c^{\dagger}_{\mathbf{k}\sigma} c_{\mathbf{k}\sigma} - US \sum_{\mathbf{k},\sigma} \sigma c^{\dagger}_{\mathbf{k}+\mathbf{Q}\sigma} c_{\mathbf{k}\sigma}, \quad (2)$$

where

$$\langle \mathrm{SDW}|S^z_{\mathbf{Q}}|\mathrm{SDW}\rangle = \frac{1}{N}\sum_{\mathbf{k},\sigma}\frac{\sigma}{2}\langle \mathrm{SDW}|c^\dagger_{\mathbf{k}+\mathbf{Q}\sigma}c_{\mathbf{k}\sigma}|\mathrm{SDW}\rangle = S \tag{3}$$

is the staggered magnetization in the SDW ground state $|\mathrm{SDW}\rangle$. The Hamiltonian (2) is diagonalized by a linear transformation which leads to

$$H_{\mathrm{MF}} = {\sum_{\mathbf{k},\sigma,l}}' l E_{\mathbf{k}} \gamma^{l\dagger}_{\mathbf{k}\sigma}\gamma^{l}_{\mathbf{k}\sigma}. \tag{4}$$

The operators $\gamma^{l(\dagger)}_{\mathbf{k}\sigma}$ destroy (create) single-particle states of energy $E_{\mathbf{k}} = l\sqrt{\epsilon^2_{\mathbf{k}}+\Delta^2}$ in the upper (conduction) and lower (valence) band of the SDW state for $l=1$ and $l=-1$, respectively. In (4) and subsequent equations primed summations are restricted to the magnetic Brillouin zone, i.e., to momenta $\mathbf{k}$ with $\epsilon_{\mathbf{k}} \le 0$. $\Delta = -US$ is one half of the size of the excitation gap between the valence and conduction band. The transformation between $c_{\mathbf{k}\sigma}$ and $\gamma^l_{\mathbf{k}\sigma}$ fermion operators reads

$$\gamma^l_{\mathbf{k}\sigma} = u^l_{\mathbf{k}} c_{\mathbf{k}\sigma} + \sigma l u^{-l}_{\mathbf{k}} c_{\mathbf{k}+\mathbf{Q}\sigma}, \quad l = \pm 1, \tag{5}$$

where $u^l_{\mathbf{k}} = \sqrt{\frac{1}{2}(1 + l\epsilon_{\mathbf{k}}/E_{\mathbf{k}})}$. The SDW ground state of the Hamiltonian (4) is determined by $\gamma^{-1\dagger}_{\mathbf{k}}|\mathrm{SDW}\rangle = 0$ and $\gamma^1_{\mathbf{k}}|\mathrm{SDW}\rangle = 0$. The SDW gap parameter Δ follows from the equation $\frac{1}{N}\sum'_{\mathbf{k}}(\epsilon^2_{\mathbf{k}}+\Delta^2)^{-1/2} = \frac{1}{U}$, which is the HF self-consistency condition for the staggered magnetization. In particular, in the strong-coupling limit, i.e., for $U \gg t$, one obtains $\Delta = U/2$.

The causal c-electron one-particle Green's function in the SDW state is given by

$$G^0_\sigma(\mathbf{k},\mathbf{k}';\omega) = \begin{bmatrix} G^0_\sigma(\mathbf{k},\mathbf{k};\omega) & G^0_\sigma(\mathbf{k},\mathbf{k}+\mathbf{Q};\omega) \\ G^0_\sigma(\mathbf{k}+\mathbf{Q},\mathbf{k};\omega) & G^0_\sigma(\mathbf{k}+\mathbf{Q},\mathbf{k}+\mathbf{Q};\omega)\end{bmatrix} = \begin{bmatrix} \omega+\epsilon_{\mathbf{k}} & \sigma\Delta \\ \sigma\Delta & \omega-\epsilon_{\mathbf{k}}\end{bmatrix}\frac{1}{\omega^2 - E^2_{\mathbf{k}} + i\eta}. \tag{6}$$

The off-diagonal components of G^0_σ are a direct consequence of Umklapp scattering with wave vector $\mathbf{Q}$ from the commensurate exchange potential of the SDW state.

In contrast to the gap in the charge excitation spectrum, the broken spin-rotational symmetry leads to two degenerate gapless Goldstone modes in the MBZ in the transverse-spin channel. These spin-wave excitations are determined by the poles of the Fourier transform of the transverse-spin susceptibility $\chi^{+-}(\mathbf{q},\mathbf{q}';t) = i\langle T[S^+_{\mathbf{q}}(t)S^-_{-\mathbf{q}'}(0)]\rangle$. To obtain the collective spin dynamics one has to include residual interactions beyond the mean-field Hamiltonian (4). Here we proceed by incorporating particle-hole interactions on the level of the RPA ladder diagram series. In the limit $U \gg t$ this procedure has previously been shown to reproduce the results of linear spin-wave theory for the two-dimensional (2D) Heisenberg model.[13] Within the RPA $\chi^{+-}(\mathbf{q},\mathbf{q}';\omega)$ is given by the matrix equation

$$\chi^{\sigma-\sigma}_{\mathrm{RPA}}(\mathbf{q},\mathbf{q}';\omega) = \sum_{\mathbf{q}''}\chi^{\sigma-\sigma}_0(\mathbf{q},\mathbf{q}'';\omega)\left[1 - U\chi^{\sigma-\sigma}_0(\mathbf{q}'',\mathbf{q}';\omega)\right]^{-1}, \tag{7}$$

where $\chi^{\sigma-\sigma}_0(\mathbf{q},\mathbf{q}';\omega)$ is the bare transverse-spin susceptibility of the SDW state

$$\chi^{\sigma-\sigma}_0(\mathbf{q},\mathbf{q}';\omega) = \frac{1}{N}{\sum_{\mathbf{k}}}' \begin{bmatrix} (E_{\mathbf{k}}+E_{\mathbf{k}+\mathbf{q}})m^2_{\mathbf{k},\mathbf{k}+\mathbf{q}} & -\sigma\omega m_{\mathbf{k},\mathbf{k}+\mathbf{q}} l_{\mathbf{k},\mathbf{k}+\mathbf{q}} \\ -\sigma\omega m_{\mathbf{k},\mathbf{k}+\mathbf{q}} l_{\mathbf{k},\mathbf{k}+\mathbf{q}} & (E_{\mathbf{k}}+E_{\mathbf{k}+\mathbf{q}})l^2_{\mathbf{k},\mathbf{k}+\mathbf{q}}\end{bmatrix}\frac{1}{(E_{\mathbf{k}}+E_{\mathbf{k}+\mathbf{q}})^2 - \omega^2 - i\eta} \tag{8}$$

with the coherence factors $m_{\mathbf{k},\mathbf{k}+\mathbf{q}} = u^1_{\mathbf{k}}u^1_{\mathbf{k}+\mathbf{q}} + u^{-1}_{\mathbf{k}}u^{-1}_{\mathbf{k}+\mathbf{q}}$ and $l_{\mathbf{k},\mathbf{k}+\mathbf{q}} = u^1_{\mathbf{k}}u^{-1}_{\mathbf{k}+\mathbf{q}} + u^{-1}_{\mathbf{k}}u^1_{\mathbf{k}+\mathbf{q}}$.

III. THE SCBA DYSON EQUATION

As in the polaron problem, we assume that the important contributions to the renormalization of the one-particle spectrum arise from the coupling to multiple low-energy-spin wave excitations. This amounts to a summation of the "rainbow" diagrams shown in Fig. 1 and leads to the self-energy equations of the so-called self-consistent Born approximation (SCBA). In the finite-temperature formalism the self-energy matrix is given by[10]

$$\Sigma_\sigma(\mathbf{k},\mathbf{k}';i\epsilon_\mu) = -TU^2\frac{1}{N}\sum_{\mathbf{q},\mathbf{q}'}\sum_{\omega_\nu} G_{-\sigma}(\mathbf{k}-\mathbf{q},\mathbf{k}'-\mathbf{q}';i\epsilon_\mu - i\omega_\nu)\chi^{-\sigma\sigma}_{\mathrm{RPA}}(\mathbf{q},\mathbf{q}';i\omega_\nu), \tag{9}$$

where $\omega_\nu = 2\pi\nu T$ and $\epsilon_\mu = (2\mu+1)\pi T$ are bosonic and fermionic Matsubara frequencies, respectively. The Green's function G_σ depends on the self-energy Σ_σ via Dyson's equation defining the self-consistency of the SCBA. The

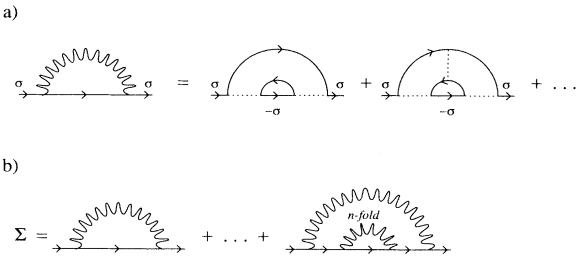

FIG. 1. (a) One-loop self-energy correction from the coupling to transverse spin fluctuations in the RPA ladder series. (b) Self-energy of the integral equation (9). The double line represents the renormalized Green's function.

summation over $\mathbf{q}'$ in Eq. (9) is restricted to $\mathbf{q}' = \mathbf{q}$ and $\mathbf{q} + \mathbf{Q}$. We perform the frequency summation and proceed via an analytic continuation to the retarded self-energy. In the zero-temperature limit we obtain the SCBA equation

$$\Sigma_\sigma(\mathbf{k},\mathbf{k}';\omega+i\eta) = U^2 \frac{1}{N\pi} \sum_{\mathbf{q}\neq\mathbf{0},\mathbf{q}'} \frac{1}{2} \int_{-\infty}^{\infty} d\nu' \int_{-\infty}^{\infty} d\nu [\mathrm{sign}(\nu') + \mathrm{sign}(\nu)] \frac{A_{-\sigma}(\mathbf{k}-\mathbf{q},\mathbf{k}'-\mathbf{q}';\nu') \mathrm{Im}[\chi^{-\sigma\sigma}_{\mathrm{RPA}}(\mathbf{q},\mathbf{q}';\nu+i\eta)]}{\nu+\nu'-\omega-i\eta} \tag{10}$$

with the spectral function $A_\sigma(\mathbf{k},\mathbf{k}';\omega) = -\mathrm{Im}[G_\sigma(\mathbf{k},\mathbf{k}',\omega+i\eta)]/\pi$. It is sufficient to calculate only two components of the self-energy, i.e., $\Sigma_\sigma(\mathbf{k},\mathbf{k};\omega+i\eta)$ and $\Sigma_\sigma(\mathbf{k},\mathbf{k}+\mathbf{Q};\omega+i\eta)$. As a consequence of the particle-hole symmetry of the Hubbard model on bipartite lattices the other two components follow from the relations $\Sigma_\sigma(\mathbf{k}+\mathbf{Q},\mathbf{k}+\mathbf{Q};z) = -\Sigma_\sigma(\mathbf{k},\mathbf{k};-z)$ and $\Sigma_\sigma(\mathbf{k}+\mathbf{Q},\mathbf{k};z) = \Sigma_\sigma(\mathbf{k},\mathbf{k}+\mathbf{Q};z)$.

In the formal limit of strong coupling, $U \gg t$, the Dyson equation (10) has previously been shown to simplify considerably.[10] The reason is that in this limit an expansion of $\chi_0^{+-}(\mathbf{q},\mathbf{q}';\omega)$ up to second order in $\frac{\omega}{U}$ and $\frac{t}{U}$ leads to an analytic expression for the RPA transverse susceptibility:[9]

$$\chi^{\sigma-\sigma}_{\mathrm{sc}}(\mathbf{q},\mathbf{q}';\omega) = \lim_{U\gg t,\omega} \chi^{\sigma-\sigma}_{\mathrm{RPA}}(\mathbf{q},\mathbf{q}';\omega) \tag{11}$$

$$= \frac{1}{\omega^2 - (\omega^{\mathrm{sw}}_{\mathbf{q}})^2 + i\eta} \begin{bmatrix} -2J(1+\epsilon_{\mathbf{q}}/4t) & \sigma\omega \\ \sigma\omega & -2J(1-\epsilon_{\mathbf{q}}/4t) \end{bmatrix} \tag{12}$$

with $J = 4t^2/U$. In this limiting form of $\chi^{\sigma-\sigma}_{\mathrm{sc}}(\mathbf{q},\mathbf{q}';\omega)$ particle-hole excitations are completely removed and the resulting susceptibility explicitly displays propagating spin waves with a dispersion $\omega^{\mathrm{sw}}_{\mathbf{q}} = 2J\sqrt{1-(\epsilon_{\mathbf{q}}/4t)^2}$. This dispersion is identical to the result of linear spin wave theory for the spin-$\frac{1}{2}$ antiferromagnetic Heisenberg model with exchange constant J. With χ_{sc} replacing χ_{RPA} in the SCBA equations, the self-energy and the Green's function matrix is most conveniently expressed with respect to the SDW conduction and valence-band particles $\gamma^1_{\mathbf{k}\sigma}$ and $\gamma^{-1}_{\mathbf{k}\sigma}$, respectively. Replacing the transformation coefficients by their strong-coupling limit, $u^l_{\mathbf{k}} = 1/\sqrt{2}$, leads to an integral equation for the γ-particle self-energy $\Sigma^\gamma_\sigma(\mathbf{k};\omega)$. Explicitly for momentum $\mathbf{k}$ in the MBZ the diagonal components of the γ-self-energy are given by

$$\Sigma^{ll}_{\gamma\sigma}(\mathbf{k};\omega+i\eta) = U^2 \frac{1}{N} {\sum_{\mathbf{q}\neq\mathbf{0}}}' \left\{ \left(1+\frac{2J}{\omega^{\mathrm{sw}}_{\mathbf{q}}}\right) \int_0^{\infty} d\nu \frac{A^{ll}_{\gamma-\sigma}(\mathbf{k}-\mathbf{q};\nu)}{\omega^{\mathrm{sw}}_{\mathbf{q}}+\nu+\omega+i\eta} + \left(1-\frac{2J}{\omega^{\mathrm{sw}}_{\mathbf{q}}}\right) \int_{-\infty}^{0} d\nu \frac{A^{ll}_{\gamma-\sigma}(\mathbf{k}-\mathbf{q};\nu)}{\omega^{\mathrm{sw}}_{\mathbf{q}}-\nu-\omega-i\eta} \right\}. \tag{13}$$

Because of the absence of excitations between the upper and lower SDW band in the strong-coupling limit, the off-diagonal parts of the γ-self-energy and the γ-Green's function vanish identically. Thus, only one equation remains for each diagonal component of the self-energy matrix which are related by $\Sigma^{-1-1}_{\gamma\sigma}(z) = -\Sigma^{11}_{\gamma\sigma}(z)$.

Single-particle spectra which have been obtained from (13) show a considerable redistribution of spectral weight from the quasiparticle peak of the SDW state into an incoherent background, both above and below the renormalized SDW energy gap.[10] This effect is due to the self-consistency of Eqs. (10) and (13). The appearance of this spin-wave shakeoff structure is strongest at the center of the MBZ. Using the renormalized quasiparticle energies

as obtained from (13) it was found that the degeneracy of the bare SDW quasiparticle energies along the border of the MBZ is barely lifted in the strong-coupling limit, with the maximum occurring at $\mathbf{k} = (0, \pi)$ and its equivalent points in the MBZ.[10] This is intriguing since it is at variance with results for the t-J model[11,3] where the maximum occurs at $\mathbf{k} = (\pm\frac{\pi}{2}, \pm\frac{\pi}{2})$. For $U = 4t$ the width of the renormalized valence band was found to be renormalized to $W = 1.85t$ in comparison to the bare SDW value of $W_{\mathrm{SDW}} = 2.81t$.

For weak or intermediate values of U the strong-coupling approximation is not justified and the complete coupled self-energy equations (10) have to be solved. In particular, interband excitations lead to the appearance of off-diagonal components in the matrix Green's function. Furthermore the full momentum dependence of the coherence factors has to be taken into account. The consequences of both, in comparison to the previous strong coupling results of Ref. 10 will be discussed in the next chapter.

IV. RESULTS AND DISCUSSION

We have solved the self-energy equations (10) numerically on finite lattices of up to 20×20 sites by iteration, starting from the HF-Green's-function matrix (6). For the frequency mesh we chose 1000 equally spaced points in the interval $[-10t, 10t]$. In all calculations an imaginary part $i\eta$ of 0.7 times the frequency spacing was introduced as an artificial broadening. To check for convergence a Lorentzian function is fitted to the highest peak in the spectra, providing its location, width and spectral weight. The spectral weight is a sensitive indication for convergence. Up to 21 iterations were necessary to achieve a stable solution with spectral changes of less than 1% between subsequent iterations. The spectral weight of the quasiparticles scales to a good approximation as const$+\frac{1}{N}$ where N is the linear dimension of the $N \times N$ lattice.

In Fig. 2 we show results for the single-hole spectral function $A_\gamma^{-1-1}(\mathbf{k};\omega)$ for $\mathbf{k}_m = (\frac{\pi}{2}, \frac{\pi}{2})$ and $\mathbf{k}_c = (0,0)$ and for $U = 4t$ on a 20×20 lattice. In Fig. 2(a) a dominant quasiparticle peak is clearly identified near the lower edge of the renormalized SDW energy gap. No such quasiparticle peak can be identified unambiguously in Fig. 2(b) for $\mathbf{k} = \mathbf{k}_c$. Similar to the spectra of the strong-coupling limit discussed before there is a considerable shift of spectral weight into the incoherent part of the spectrum. The actual amount of this shift is, however, drastically enhanced due to particle-hole excitations across the SDW energy gap when compared to the strong-coupling approximation for the same momenta and coupling strength U/t.

Figure 3 shows the quasiparticle dispersion on a closed path in the MBZ with a distinct maximum at $\mathbf{k}_m$ and a flat part around $(0, \pi)$. This is consistent with results obtained for the t-J model within a similar SCBA approach for the self-energy,[11] with Green's-function Monte Carlo results for the t-J model,[14] with quantum Monte Carlo results for the Hubbard model,[15,16] and with recent results on the three-band Hubbard model using a conserving approximation including spin and charge fluctuations.[17] The maximum occurs at $\mathbf{k}_m$ for all values of the interaction investigated, i.e., for $3.0t < U < 5.5t$. The excitation gap is found to be strongly renormalized by a factor of ≈ 0.25 to $\Delta_r = 0.36t$ as compared to the bare SDW value $\Delta_{\mathrm{SDW}} = 1.39t$. Similarly, the width of the quasiparticle band is strongly reduced by a factor

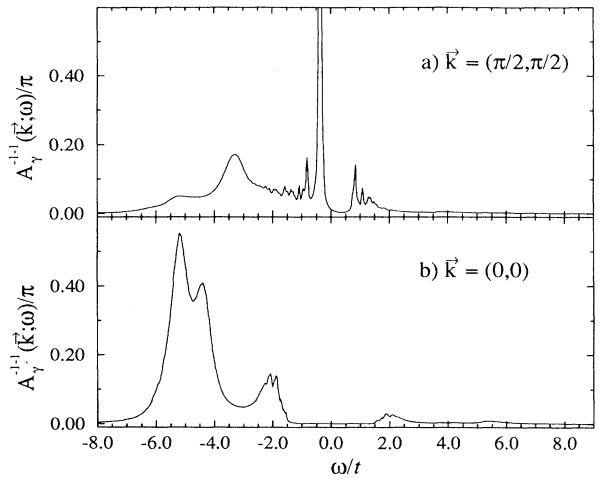

FIG. 2. Single-hole spectral function $A_\gamma^{-1-1}(\mathbf{k};\omega)$ for $U = 4t$ and the two momenta (a) $\mathbf{k} = (\frac{\pi}{2}, \frac{\pi}{2})$ and (b) $\mathbf{k} = (0,0)$ on a 20×20 lattice. Energies are given in units of t.

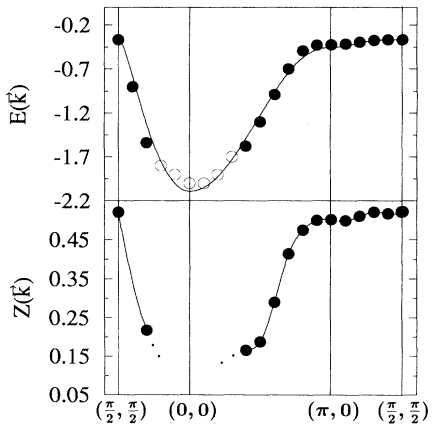

FIG. 3. (a) Quasiparticle dispersion for $U = 4t$ on a 20×20 lattice along a closed path in the MBZ. The values for the energies and the spectral weight of the quasiparticles were obtained by fitting a Lorentzian function to the quasiparticle peak. Solid circles show the quasiparticle energies as obtained from the SCBA spectra for cases of a well-defined quasiparticle peak. Open circles denote momenta near the center of the MBZ where a unique determination of the quasiparticle energies is not possible. The solid line represents the fitted dispersion $E'_{\mathbf{k}} = \sqrt{\Delta_r^2 + [2\tilde{t} \cdot (\cos k_x + \cos k_y) + 4t' \cdot \cos k_x \cos k_y]^2}$ with $\tilde{t} = 0.583t$ and $t' = -0.0675t$. (b) Dispersion of the quasiparticle weight along the same path as in (a). The quasiparticle weights for momenta without a unique quasiparticle energy have been omitted.

0.58 to $1.64t$.

As a guiding criterion to identify the location of the quasiparticle peak near the center of the MBZ we have assumed a continuous quasiparticle dispersion. The quasiparticle dispersion near $\mathbf{k}_c$ is then obtained by tracing the quasiparticle energies from the boundary of the MBZ to its center. The quasiparticle energy and its spectral weight at the boundary of the MBZ is unambiguous, while a quasiparticle peak near the center of the MBZ can only be resolved with the assumption of a continuous dispersion. The quasiparticle weight is also given in Fig. 3 and shows a dispersion similar to the energies. Extrapolation of the finite size behavior of the quasiparticle weight at $\mathbf{k}_m$ to infinite lattices would yield a value of $Z(\mathbf{k}_m) \approx 0.42$.

Figure 3 also displays a dispersion fitted to the quasiparticle energies for $U = 4.0t$. It includes next-nearest-neighbor hopping on the two sublattices of the commensurate SDW state. Explicitly, the dispersion has been fitted by the expression

$$E'_{\mathbf{k}} = -\sqrt{\Delta_r^2 + [2\tilde{t} \cdot (\cos k_x + \cos k_y) + 4t' \cdot \cos k_x \cos k_y]^2}. \tag{14}$$

This approximated dispersion accounts rather well for the form of the dispersion along the boundary of the MBZ. The fit parameters are $\tilde{t} = 0.583t$ and $t' = -0.0675t$. The maximum at $\mathbf{k}_m$ and the flat region around $(0, \pi)$ are well described by $E'_{\mathbf{k}}$. The small but finite parameter t' for next-nearest-neighbor hopping implies that the spin-wave dressing generates an effective hopping within the two sublattices which allows for electronic motion without disturbing the AF order of the SDW state. Figure 4 shows a contour plot of the dispersion $E'_{\mathbf{k}}$ with pocketlike features near $(\pm\frac{\pi}{2}, \pm\frac{\pi}{2})$, suggesting that the Fermi surface will maintain pocketlike structures also at small but finite doping.

Finally we show in Fig. 5 the density of states, $N(\omega) = \frac{1}{N}\sum'_{\mathbf{k},l=\pm1} A^{ll}_{\gamma}(\mathbf{k};\omega)$ for $U = 4t$, as obtained from the solution of the SCBA self-energy equations (a) and for the initial SDW state (b). The comparison between (a) and (b) illustrates the significant renormalization of the excitation gap. Furthermore (a) shows that there are three different contributions to the spectral weight. There are narrow quasiparticle valence and conduction bands with bandwidth $W = 1.64t$ separated by a renormalized excitation gap of $\Delta_r = 0.72t$. On a scale set by the spin-wave energy the quasiparticle weight is redistributed into spin-wave shakeoff structures. Additionally there are broad peaks with a maximum at $\pm 3.8t$. These shakeoff features result from the coupling of the quasiparticle to interband particle-hole excitations across the SDW energy gap and appear at energies of 2Δ above (below) the conduction (valence) quasiparticle band. For intermediate and large values of U/t this energy scale is set by the Hubbard interaction U itself and the broad peaks in Fig. 5 at $\pm 3.8t$ therefore resemble the upper and lower Hubbard band. A similar qualitative picture has recently been developed for the interpretation of quantum Monte Carlo results for the 2D half-filled Hubbard model.[18]

Figure 6 shows spectra by Dagotto, Ortolani, and Scalapino[15] obtained by exact diagonalization using the Lanczos algorithm for $U = 8t$ on a 4×4 lattice in comparison with our SCBA results for the same lattice size and the same interaction strength U/t. All spectra are given in c-particle representation. For the weak-coupling SCBA analysis this is a rather large interaction, but for smaller values of U no exact results are available to compare with. Concerning the energy, width and spectral weight of the quasiparticle at $\mathbf{k} = (0, \pi)$ and $\mathbf{k} = (0, \frac{\pi}{2})$ both spectra are quite similar. The excitation gap of the

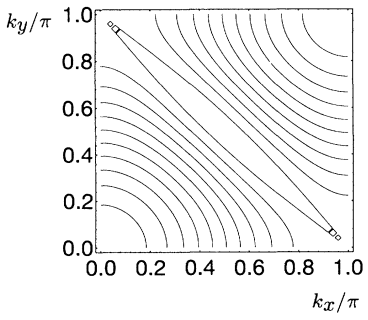

FIG. 4. Contour plot of the fit $E'_{\mathbf{k}}$ [Eq. (14) and Fig. 3] to the quasiparticle dispersion for $U = 4t$ on a 20×20 lattice.

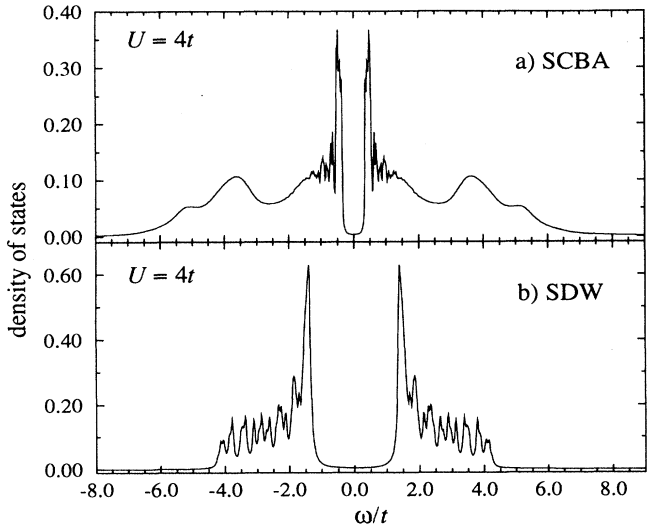

FIG. 5. Comparison of the density of states as obtained from the SCBA spectra for $U = 4t$ on a 20×20 lattice (a) with the bare SDW density of states for the same parameters (b).

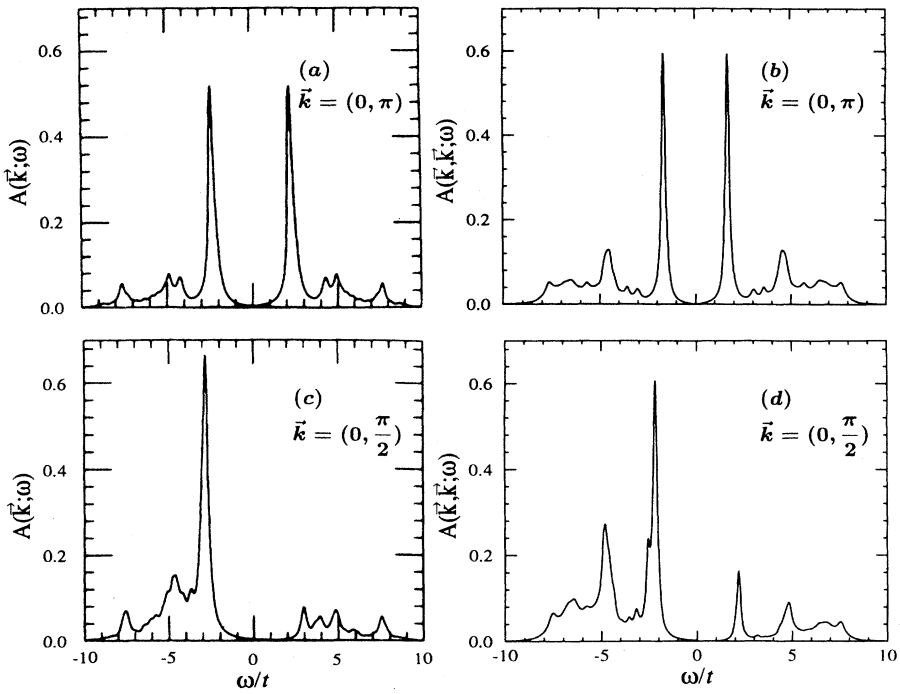

FIG. 6. (a) and (c) show spectra for $U = 8t$ on a 4×4 lattice at half-filling obtained via exact diagonalization using the Lanczos algorithm (Ref. 15) (reproduction with the kind permission of Dagotto), the spectra in (b) and (d) are results from solving the SCBA self-energy equations, given in c-particle representation for momenta $\mathbf{k} = (0, \pi)$ and $\mathbf{k} = (0, \frac{\pi}{2})$, respectively.

Lanczos density of states is 15% larger than in the SCBA calculations. This discrepancy is not too surprising since the weak-coupling SCBA calculation is not expected to give quantitatively reliable results for U as large as $8t$. Yet, the qualitative and even quantitative agreement to the Lanczos data is remarkable.

The comparison of the results from solving the complete self-energy equations to the results obtained in the strong-coupling limit of the SCBA equations[10] exhibits several differences. As mentioned before, in the strong-coupling limit the maximum of the quasiparticle dispersion is located at $(0, \pi)$ and the degeneracy along the border of the MBZ was found to be barely lifted. In contrast the solution of the complete SCBA equations yields a distinct maximum at $(\frac{\pi}{2}, \frac{\pi}{2})$. Due to neglecting interband excitations and the momentum dependence of the coherence factors, the renormalization effects turn out weaker in the strong-coupling limit. The reduction of the excitation gap, the bandwidth, and the spectral weight of the quasiparticle peak is larger when using the complete self-energy equations.

In summary we have calculated the single-particle spectral function of the Hubbard model at half-filling starting from the weak-coupling SDW state. Our self-consistent ansatz for the self-energy accounts for multiple exchange of low-energy transverse-spin excitations. A comparison to exact diagonalization results and self-consistent calculations in the t-J model show that the single-particle properties up to moderate values of the interaction are well described within this approximation. The comparison to the previous simplified SCBA analysis in the strong-coupling limit reveals the importance to take into account the full SCBA self-energy equations. Large renormalization effects and redistribution of spectral weight are found within the self-consistent SCBA calculations even at weak-coupling values of U/t.

ACKNOWLEDGMENTS

This work has been performed within the program of the Sonderforschungsbereich 341 supported by the Deutsche Forschungsgemeinschaft (DFG). A.P.K. gratefully acknowledges the support through the Heisenberg foundation of the DFG. We also acknowledge useful correspondence and discussion with E. Dagotto.

[1] For recent reviews, see E. Dagotto, Rev. Mod. Phys. **66**, 763 (1994); A.P. Kampf, Phys. Rep. **249**, 219 (1994); W. Brenig, *ibid.* **251**, 153 (1995).

[2] C. Kane, P. Lee, and N. Read, Phys. Rev. B **39**, 6880 (1989).

[3] F. Marsiglio, A.E. Ruckenstein, S. Schmitt-Rink, and C.M. Varma, Phys. Rev. B **43**, 10 882 (1991).

[4] G. Martinez and P. Horsch, Phys. Rev. B **44**, 317 (1991).

[5] W. Stephan and P. Horsch, Phys. Rev. B **42**, 8736 (1990); E. Dagotto, E.A. Morea, F. Ortolani, J. Riera, and D.J.

Scalapino, *ibid.* **45**, 10 107 (1992); A.P. Kampf and W. Brenig, J. Low Temp. Phys. **95**, 329 (1994).
[6] T. Uchida, T. Ido, H. Takagi, T. Arima, Y. Tokura, and S. Tajima, Phys. Rev. B **43**, 7942 (1991).
[7] A.V. Chubukov and D.M. Frenkel, Phys. Rev. B **46**, 11 884 (1992).
[8] A. Vignale and M.R. Hedayati, Phys. Rev. B **42**, 786 (1990).
[9] A. Singh and Z. Tešanović, Phys. Rev. B **41**, 614 (1990).
[10] W. Brenig and A.P. Kampf, Europhys. Lett. **24**, 679 (1993).
[11] J. Igarashi and P. Fulde, Phys. Rev. B **48**, 998 (1993).
[12] J. Hubbard, Proc. R. Soc. London Ser. A **276**, 283 (1963); M. Gutzwiller, Phys. Rev. Lett. **10**, 159 (1963); J. Kanamori, Prog. Theor. Phys. **30**, 275 (1963).
[13] J.R. Schrieffer, X.G. Wen, and S.C. Zhang, Phys. Rev. B **39**, 11 663 (1989).
[14] E. Dagotto, A. Nazarenko, and M. Boninsegni, Phys. Rev. Lett. **73**, 728 (1994).
[15] E. Dagotto, F. Ortolani, and D.J. Scalapino, Phys. Rev. B **46**, 3183 (1992).
[16] N. Bulut, D.J. Scalapino, and S.R. White, Phys. Rev. B **50**, 9623 (1994).
[17] R. Putz, R. Preuss, A. Muramatsu, and W. Hanke (unpublished).
[18] R. Preuss, W. Hanke, and W. von der Linden (unpublished).